University of Central Lancashire UCLan

Central Lancashire Online Knowledge (CLoK)

Title	4-Nonylphenol effects on rat testis and sertoli cells determined by spectrochemical techniques coupled with chemometric analysis
Type	Article
URL	https://clok.uclan.ac.uk/id/eprint/24909/
DOI	https://doi.org/10.1016/j.chemosphere.2018.11.086
Date	2019
Citation	Duan, Peng, Liu, Bisen, Medeiros-De-morais, Camilo De lelis orcid iconORCID: 0000-0003-2573-787X, Zhao, Jing, Li, Xiandong, Tu, Jian, Yang, Weiyingxue, Chen, Chunling, Long, Manman et al (2019) 4-Nonylphenol effects on rat testis and sertoli cells determined by spectrochemical techniques coupled with chemometric analysis. Chemosphere, 218. pp. 64-75. ISSN 0045-6535
Creators	Duan, Peng, Liu, Bisen, Medeiros-De-morais, Camilo De lelis, Zhao, Jing, Li, Xiandong, Tu, Jian, Yang, Weiyingxue, Chen, Chunling, Long, Manman, Feng, Xiaobing, Martin, Francis L and Xiong, Chengliang

It is advisable to refer to the publisher's version if you intend to cite from the work. https://doi.org/10.1016/j.chemosphere.2018.11.086

For information about Research at UCLan please go to http://www.uclan.ac.uk/research/

All outputs in CLoK are protected by Intellectual Property Rights law, including Copyright law. Copyright, IPR and Moral Rights for the works on this site are retained by the individual authors and/or other copyright owners. Terms and conditions for use of this material are defined in the http://clok.uclan.ac.uk/policies/

Electronic Supplementary Information

4-Nonylphenol effects on rat testis and Sertoli cells determined by spectrochemical techniques coupled with chemometric analysis

Peng Duan[1,2], Bisen Liu[3], Camilo L. M. Morais[4], Jing Zhao[5], Xiandong Li[6], Jian Tu[7], Weiyingxue Yang[3], Chunling Chen[3], Manman Long[3], Xiaobing Feng[3], Francis L. Martin[4,¶], Chengliang Xiong[1,8,¶]

[1]Family Planning Research Institute, Tongji Medical College, Huazhong University of Science and Technology, Wuhan 430030, China; *[2]Center for Reproductive Medicine, Xiangyang No. 1 People's Hospital, Hubei University of Medicine, Xiangyang 441000, China*; *[3]Department of Epidemiology and Biostatistics, School of Public Health, Tongji Medical College, Huazhong University of Science and Technology, Wuhan, Hubei, China*; *[4]School of Pharmacy and Biomedical Sciences, University of Central Lancashire, Preston PR1 2HE, UK*; *[5]Department of Epidemiology and Health Statistics, School of Public Health, Medical College, Wuhan University of Science and Technology, Wuhan 430030, China*; *[6]Department of Clinical Laboratory, Taihe Hospital, Hubei University of Medicine, Shiyan 442000, China*; *[7]Reproductive medicine center, Maternal and Child Health Care Hospital of Yueyang City, Yueyang 414000, China*; *[8]Center for Reproductive Medicine, Wuhan Tongji Reproductive Medicine Hospital, 128 Sanyang Road, Wuhan 430013, China*

¶ Corresponding authors:

¶Chengliang Xiong, Family Planning Research Institute, Tongji Medical College, Huazhong University of Science and Technology, 13 Hangkong Road, 430030 Wuhan, Hubei Province, China. Tel: +86-0278-83692651; E-mail: clxiong951@sina.com.

¶Francis L. Martin, School of Pharmacy and Biomedical Sciences, University of Central Lancashire, Preston PR1 2HE, UK. Tel: +44 (0)-1772 89-6482; E-mail: flmartin@uclan.ac.uk

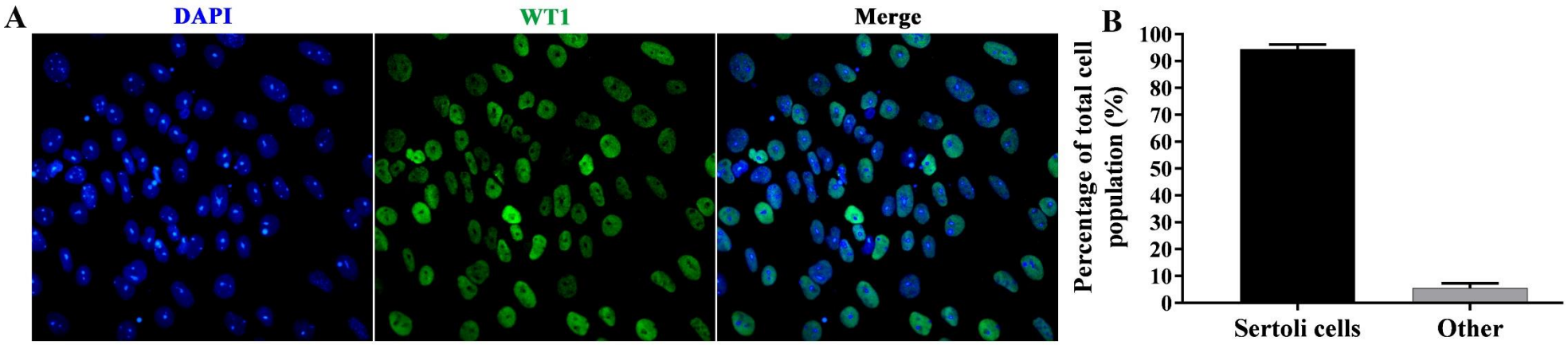

Figure S1. The purity of Sertoli cells (SCs) was assessed by immunocytochemical staining of WT1 (original magnification ×200). (A) Sertoli cells labelled by WT1 (green) immunofluorescence staining. The cell nucleus was stained with DAPI (blue). **(B)** Percentage of SCs and other cells was provided from 10 random fields in multiple coverslips. The mean percentages of SCs and other cells were 94.46% and 5.54% respectively.

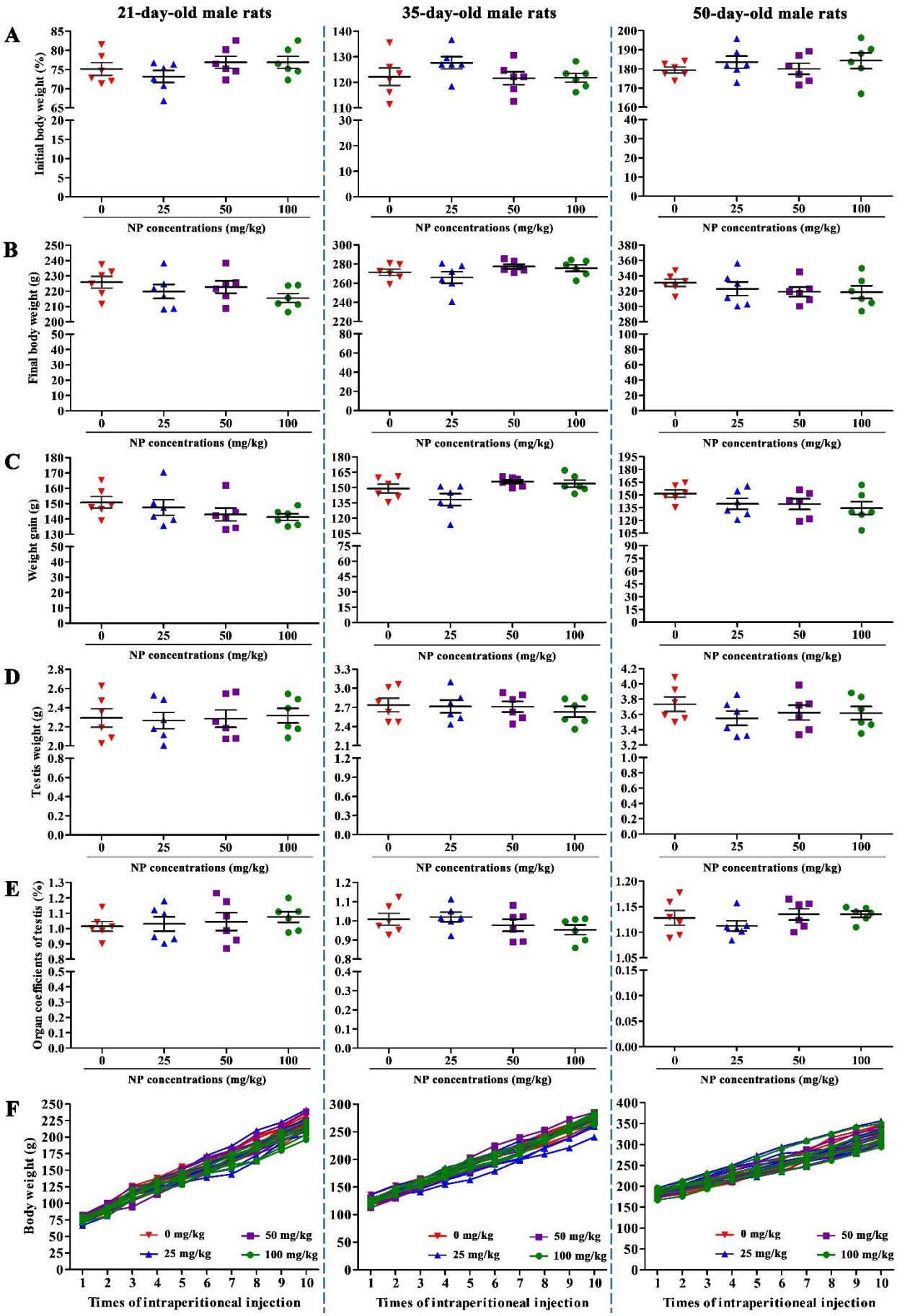
21-day-old male rats
35-day-old male rats
50-day-old male rats
A
Initial body weight (%)
B
Final body weight (g)
C
Weight gain (g)
D
Testis weight (g)
E
Organ coefficients of testis (%)
NP concentrations (mg/kg)
F
Body weight (g)
Times of intraperitioneal injection
0 mg/kg
25 mg/kg
50 mg/kg
100 mg/kg

Figure S2. Effects of 4-nonylphenol (NP) on the initial body weight, final body weight, weight gain, testis weight and organ coefficient of rat testis. (A) Comparison of initial body weight; **(B)** Comparison of final body weight; **(C)** Effects of NP on weight gain; **(D)** Effects of NP on testis weight; **(E)** Effects of NP on organ coefficient of testis; and, **(F)** Body weight of male rats during NP treatment period. First column: 21-day-old male rats; Second column: 35-day-old male rats; Third column: 50-day-old male rats. All the data are represented as mean ± standard deviations. n=6 for each group. The results of one-way ANOVA analysis showed that there was no significant differences between NP-exposed and control groups for all variables in the Figure S2 (P>0.05).

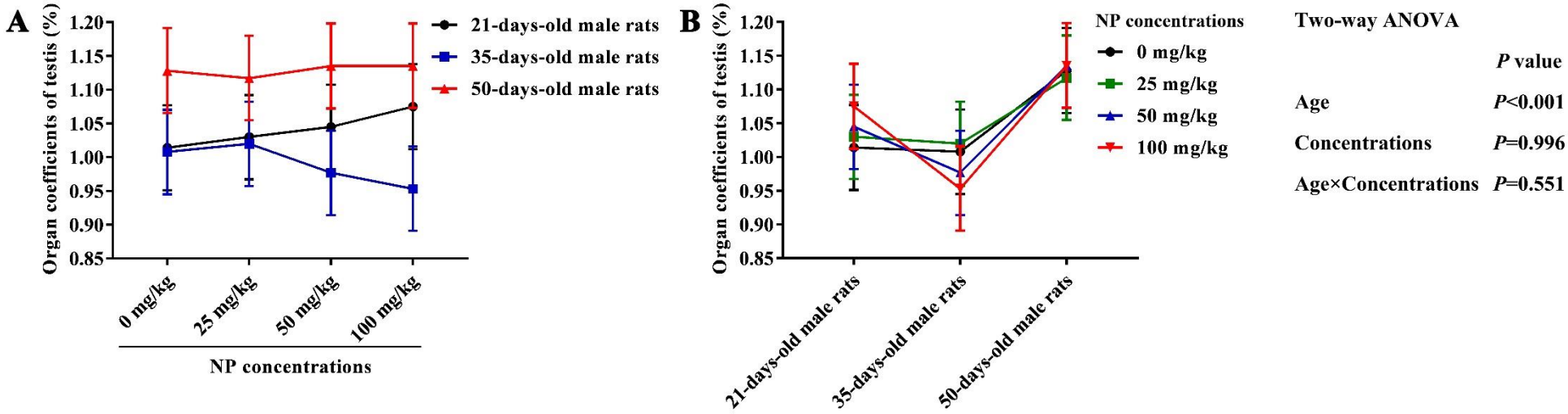

Figure S3. Organ coefficient of rat testis was analysed by two-way ANOVA to evaluate the effect of exposure age, 4-nonylphenol (NP) administration, or interaction. (A) The effect of NP-exposure life stage on organ coefficient of rat testis. **(B)** The effect of NP exposure on organ coefficient of rat testis. Data represent mean ± 95% confidence intervals.

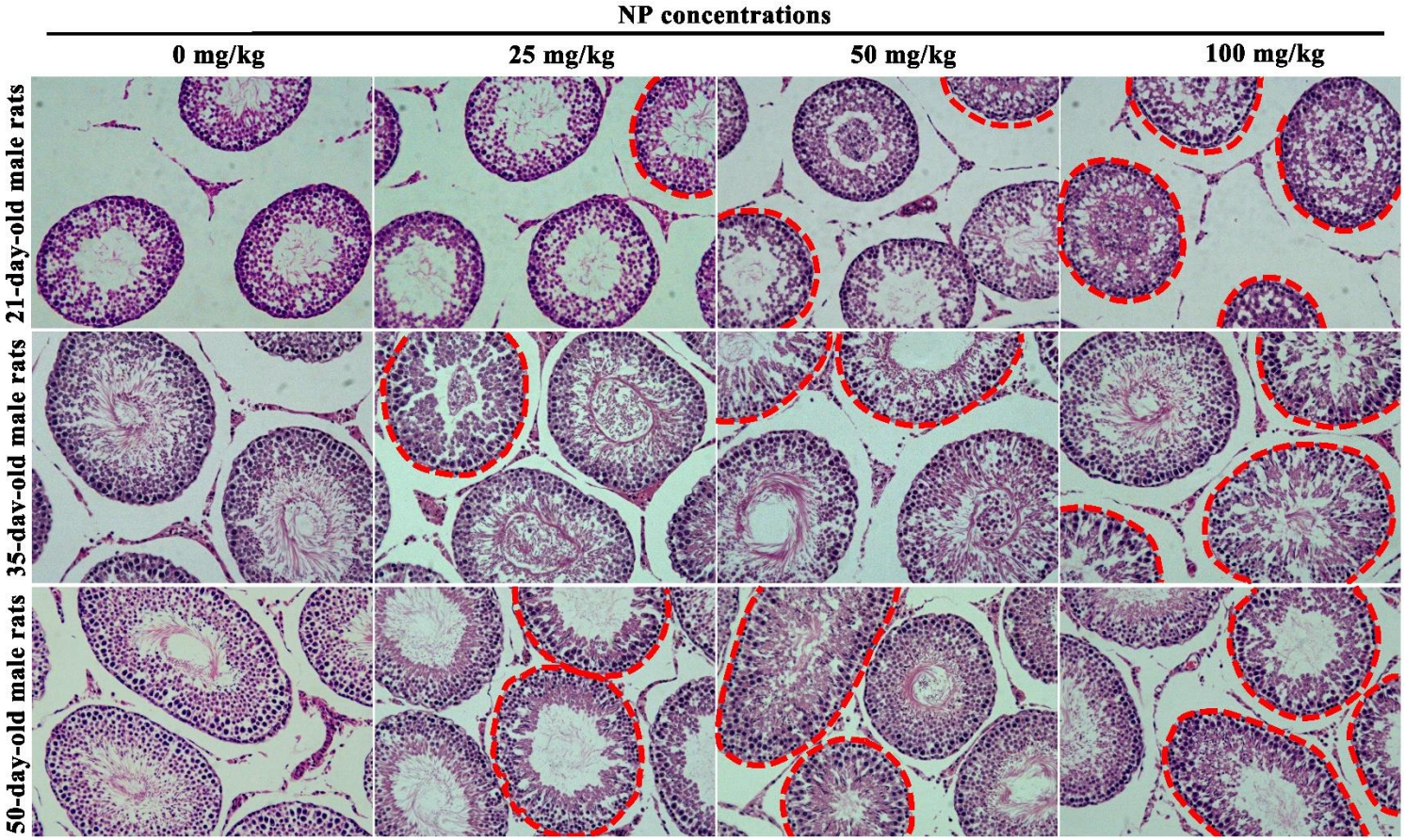

Figure S4. Representative photomicrographs of testis sections stained with haematoxylin and eosin dye (200× magnification). Seminiferous tubules with abnormal cell arrangement (indicated by red dotted circle). Top row: 21-day-old rats. Middle row: 35-day-old rats. Bottom row: 50-day-old rats.

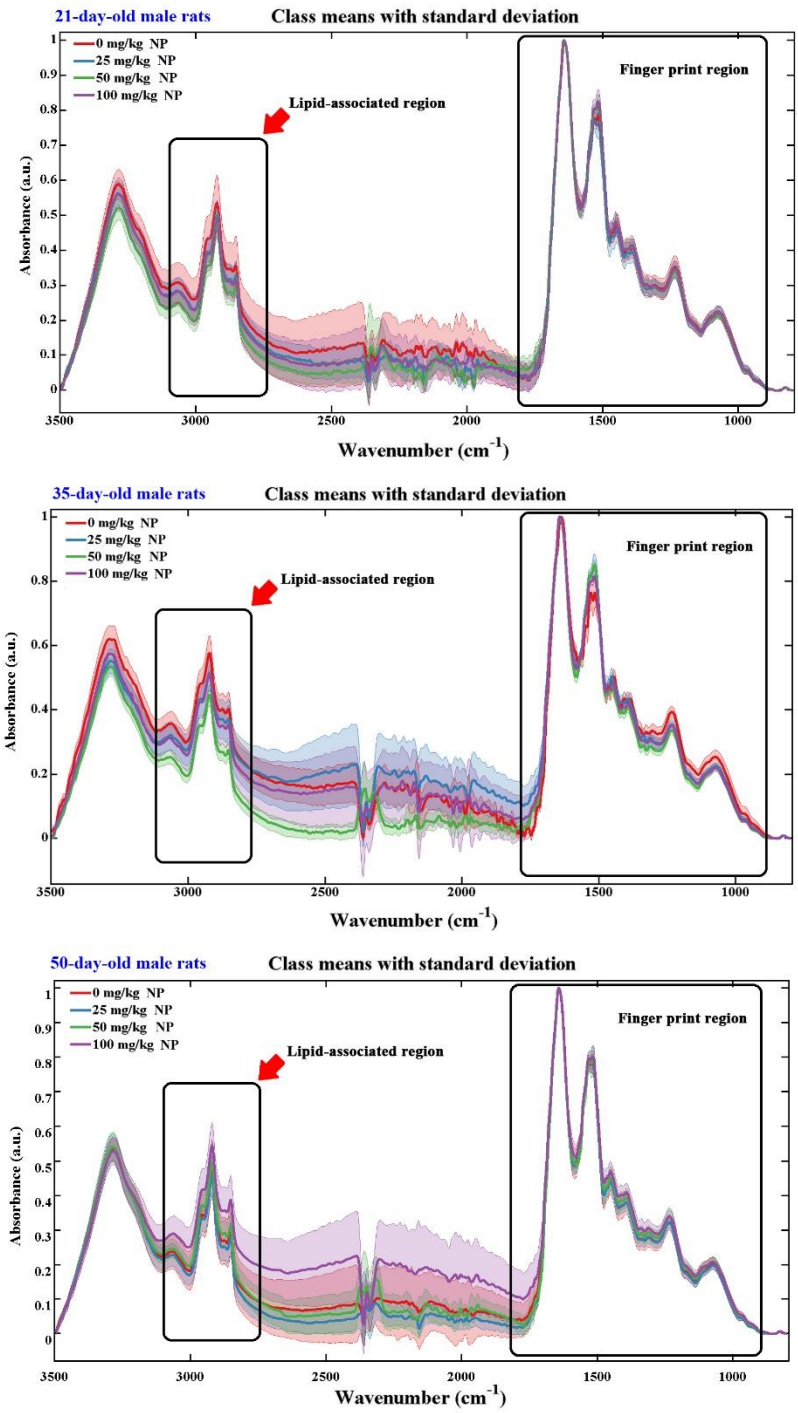

Figure S5. Mean IR spectra ± standard deviation derived in the analysis of testicular cells in the 3500-800 cm^{-1} region. The resultant IR spectra included two regions of interest at 3200-2800 cm^{-1} (CH-region: lipids) and 1800-900 cm^{-1} (biochemical-cell fingerprint region). IR spectra were baseline-corrected and normalized to the Amide I. The different categories were classified as: 0 mg/kg 4-Nonylphenol (NP) (red solid line), 25 mg/kg NP (blue solid line), 50 mg/kg NP (green solid line), and 100 mg/kg NP (purple solid line). *n*=6 for each group of rats.

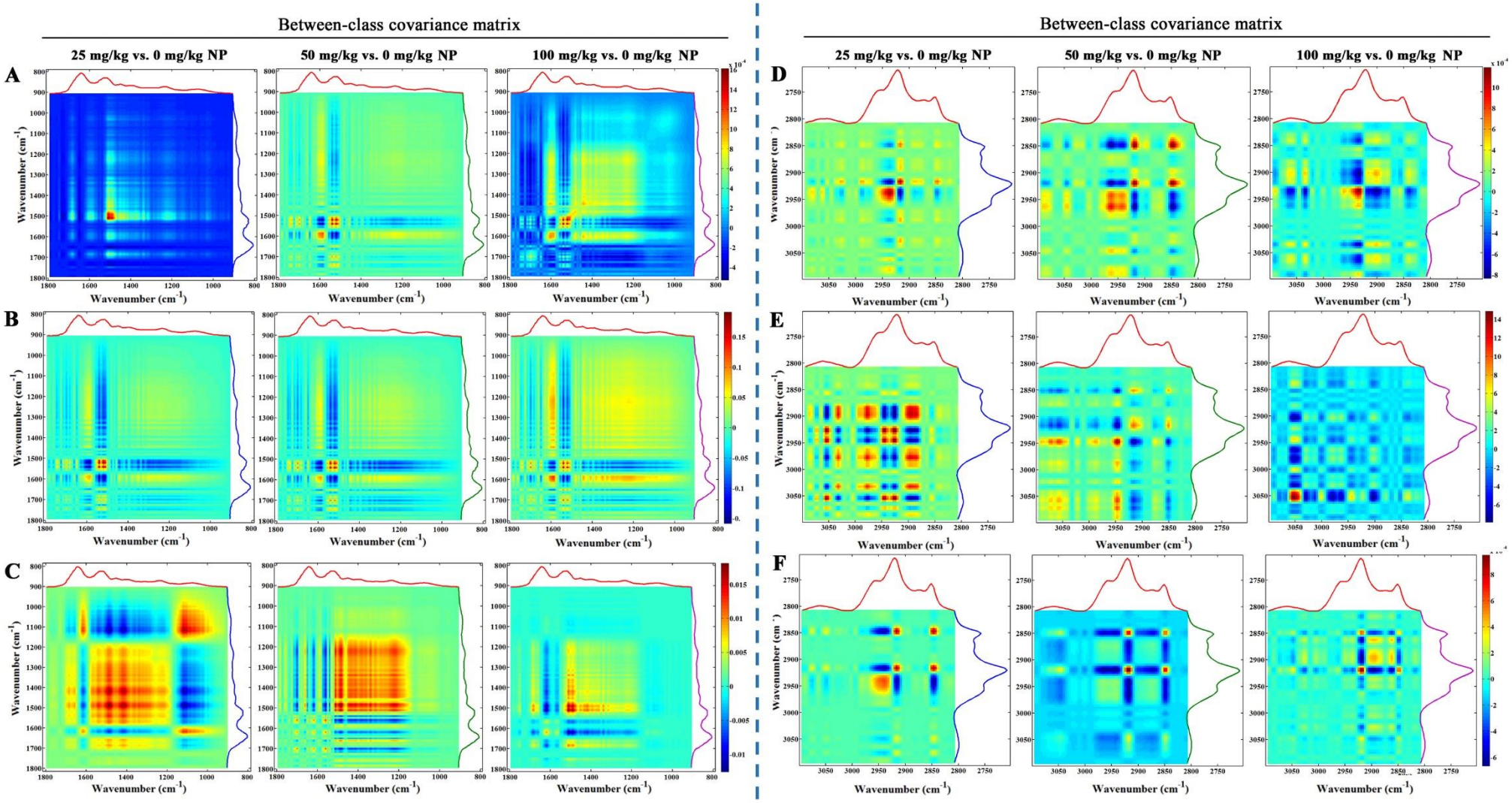
Between-class covariance matrix
25 mg/kg vs. 0 mg/kg NP
50 mg/kg vs. 0 mg/kg NP
100 mg/kg vs. 0 mg/kg NP
A
B
C
D
E
F
Wavenumber (cm-1)

Figure S6. ATR-FTIR spectroscopy-based between-class covariance matrix showing the absorbance variations of 4-nonylphenol (NP) treatment *vs.* control categories. Between-class covariance matrix of spectral region 1800-900 cm^{-1} for NP-treated 21-day-old rats **(A)**, for NP-treated 35-day-old rats **(B)** and for NP-treated 50-day-old rats **(C)**. Between-class covariance matrix of spectral region 3200-2800 cm^{-1} for NP-treated 21-day-old rats **(D)**, for NP-treated 35-day-old rats **(E)** and for NP-treated 50-day-old rats **(F)**. Between group comparison: 25 mg/kg *vs.* 0 mg/kg NP groups, 50 mg/kg *vs.* 0 mg/kg NP groups and 100 mg/kg *vs.* 0 mg/kg NP groups. Data represent the average of six mice per group.

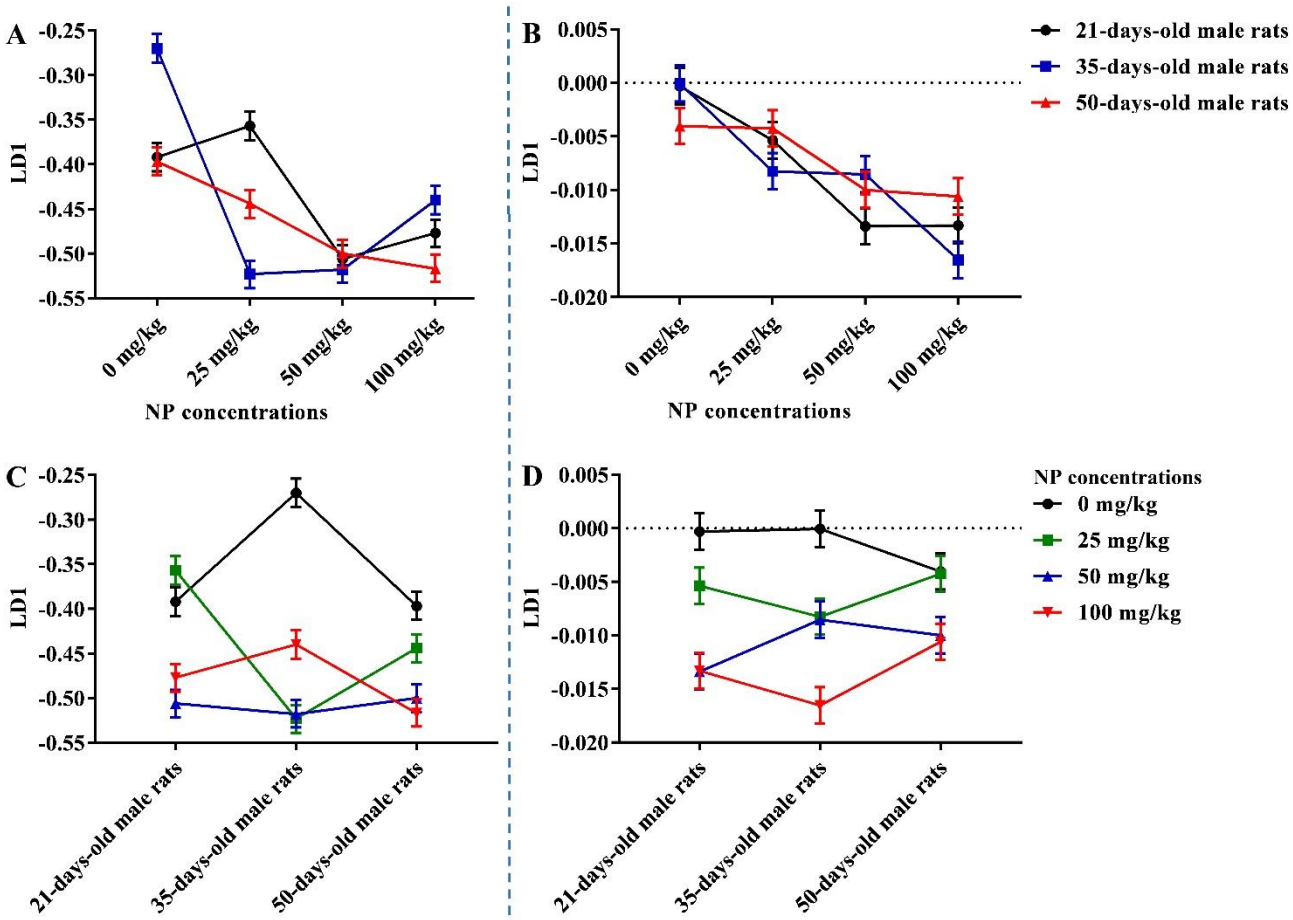

Two-way ANOVA

	P value
Age	*P*<0.001
Concentrations	*P*<0.001
Age×Concentrations	*P*<0.001

Two-way ANOVA

	P value
Age	*P*=0.154
Concentrations	*P*<0.001
Age×Concentrations	*P*<0.001

Figure S7. Linear discriminant 1 (LD1) score of IR spectra extracted from testicular cells was analysed by two-way ANOVA to evaluate the effect of exposure age, 4-nonylphenol (NP) administration, or interaction. The effects of NP-exposure on life-stage on LD1 scores of both the 1800-900 cm^{-1} region **(A)** and 3200-2800 cm^{-1} region **(B)**. The effects of NP exposure on LD1 scores of both the 1800-900 cm^{-1} region **(C)** and 3200-2800 cm^{-1} region **(D)**. Data represent mean ± 95% confidence intervals.

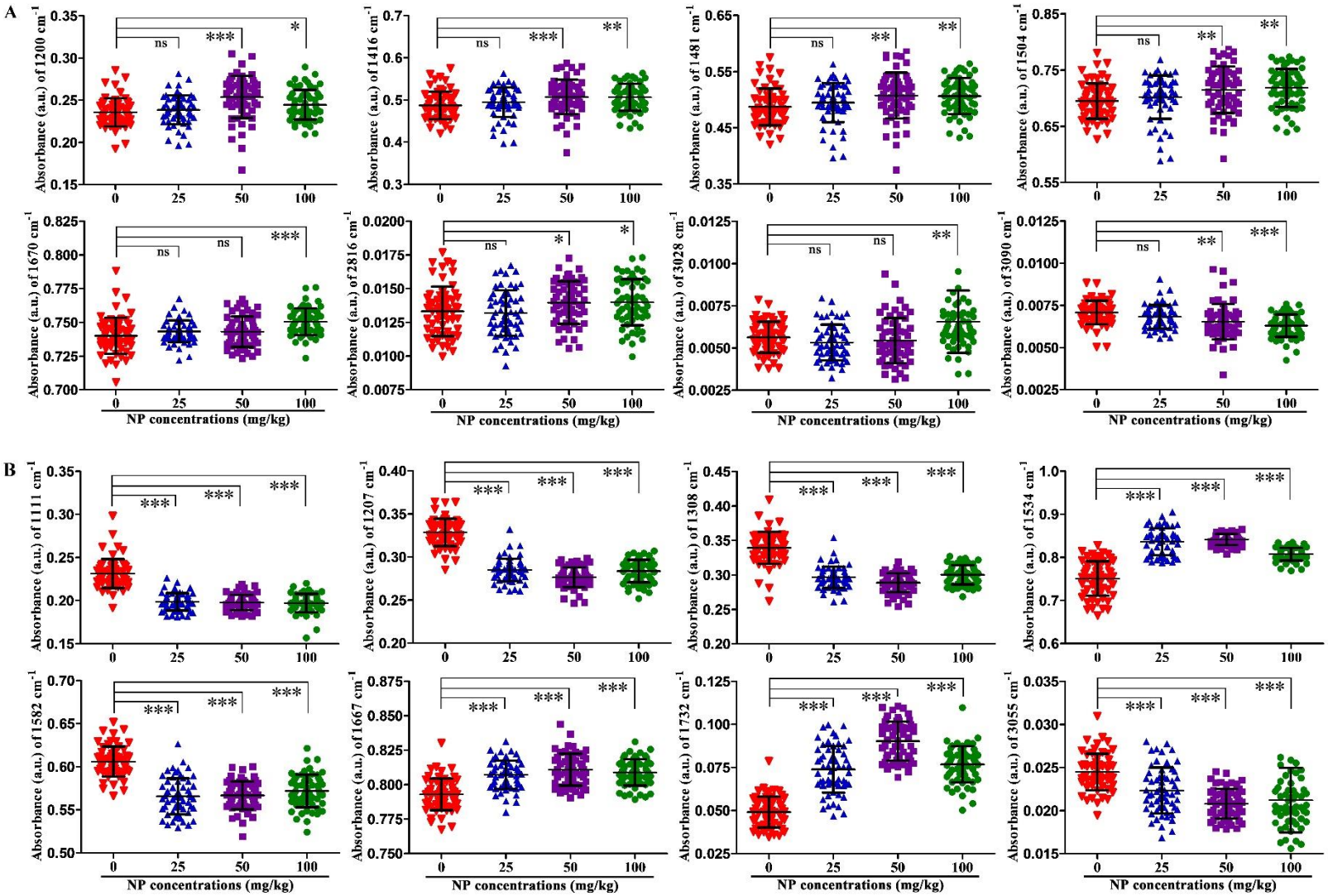
A
Absorbance (a.u.) of 1200 cm-1
Absorbance (a.u.) of 1416 cm-1
Absorbance (a.u.) of 1481 cm-1
Absorbance (a.u.) of 1504 cm-1
Absorbance (a.u.) of 1670 cm-1
Absorbance (a.u.) of 2816 cm-1
Absorbance (a.u.) of 3028 cm-1
Absorbance (a.u.) of 3090 cm-1
NP concentrations (mg/kg)
B
Absorbance (a.u.) of 1111 cm-1
Absorbance (a.u.) of 1207 cm-1
Absorbance (a.u.) of 1308 cm-1
Absorbance (a.u.) of 1534 cm-1
Absorbance (a.u.) of 1582 cm-1
Absorbance (a.u.) of 1667 cm-1
Absorbance (a.u.) of 1732 cm-1
Absorbance (a.u.) of 3055 cm-1
NP concentrations (mg/kg)

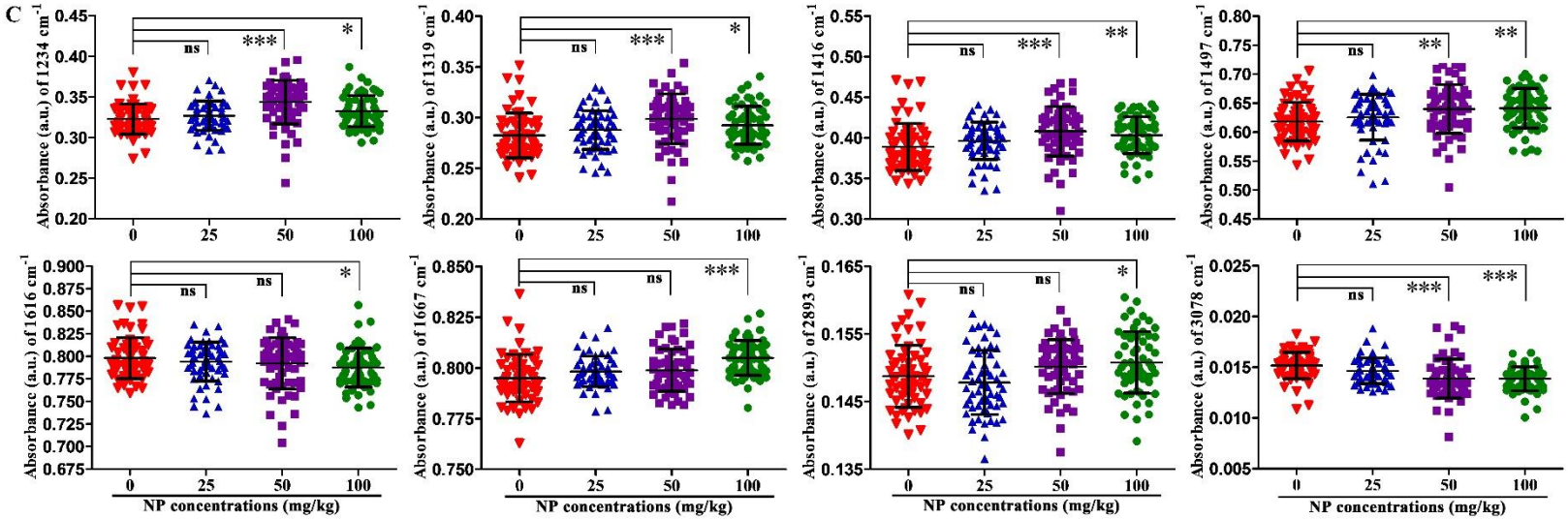

Figure S8. Variations of IR spectral absorption of discriminating wavenumbers responsible for segregation of 4-nonylphenol (NP) exposure groups. (A) Absorption variations for the bands located at the 1200, 1416, 1481, 1504, 1670, 2816, 3028 and 3090 cm^{-1} of testicular cells of NP-treated 21-day-old rats. **(B)** Absorption variations for the bands located at the 1111, 1207, 1308, 1534, 1582, 1667, 1732 and 3055 cm^{-1} of testicular cells of NP-treated 35-day-old rats. **(C)** Absorption variations for the bands located at the 1234, 1319, 1416, 1497, 1616, 1667, 2893 and 3078 cm^{-1} of testicular cells of NP-treated 50-day-old rats. All the data are represented as mean ± standard deviation, n=6 for each group. "ns" denotes no statistical significance (P>0.05); * indicates P-value of <0.05; ** indicates P-value of <0.01; *** indicates P-value of <0.001, one-way ANOVA with the Fisher's LSD or Dunnett's T3 post-hoc test.

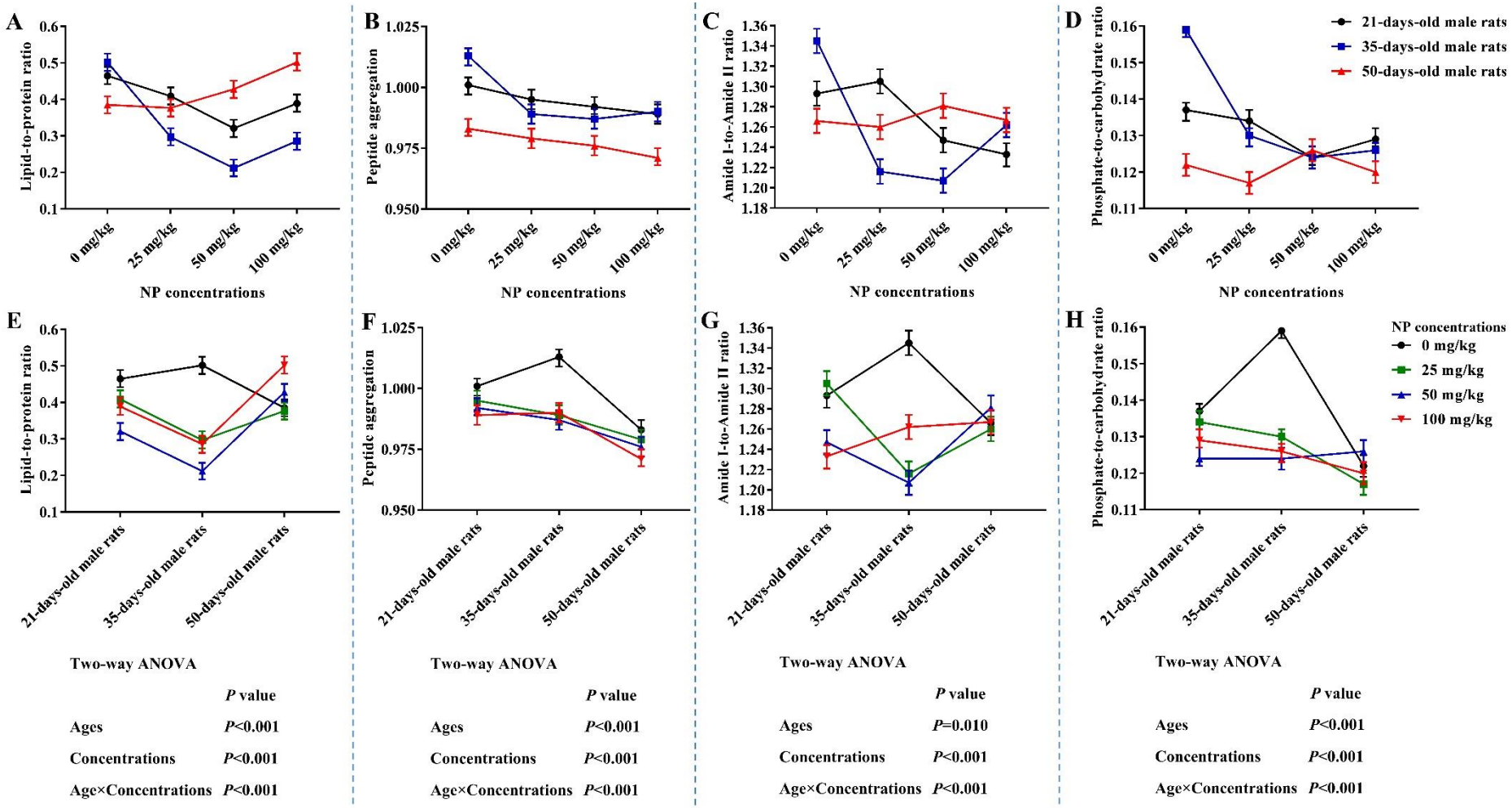

Figure S9. The ratios of lipid-to-protein, peptide aggregation, Amide I-to-Amide II ratio and phosphate-to-carbohydrate were analysed by two-way ANOVA to evaluate the effect of 4-nonylphenol (NP) administration, exposure age, or interaction. The effect of NP-exposure

life stage on lipid-to-protein ratio **(A)**, peptide aggregation **(B)**, Amide I-to-Amide II ratio **(C)**, and phosphate-to-carbohydrate ratio **(D)**. The effect of NP exposure on lipid-to-protein ratio **(E)**, peptide aggregation **(F)**, Amide I-to-Amide II ratio **(G)**, and phosphate-to-carbohydrate ratio **(H)**. Data represent mean ± 95% confidence intervals.

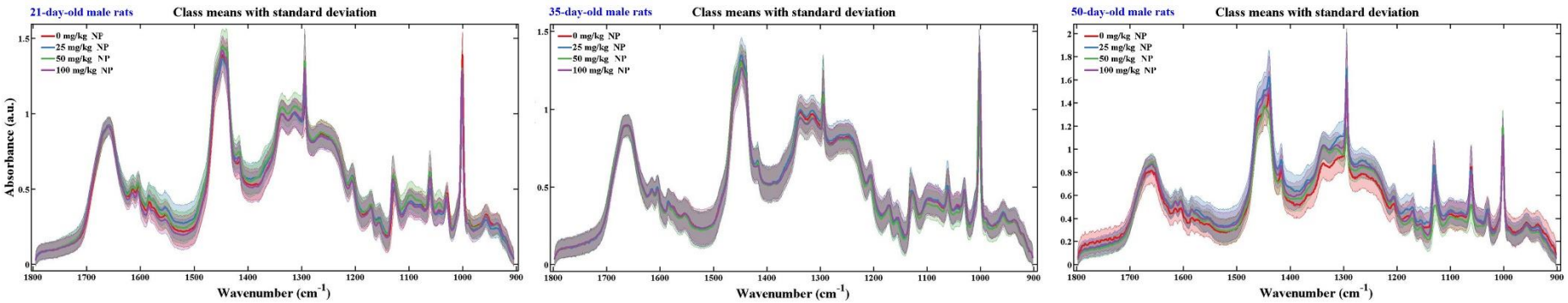

Figure S10. Mean Raman spectra ± standard deviation derived in the analysis of testicular interstitial tissue in the 1800-900 cm^{-1} region. Raman spectra were baseline-corrected and normalized to the Amide I. The different categories were classified as: 0 mg/kg 4-nonylphenol (NP) (red solid line), 25 mg/kg NP (blue solid line), 50 mg/kg NP (green solid line), and 100 mg/kg NP (purple solid line). *n*=6 for each group of rats.

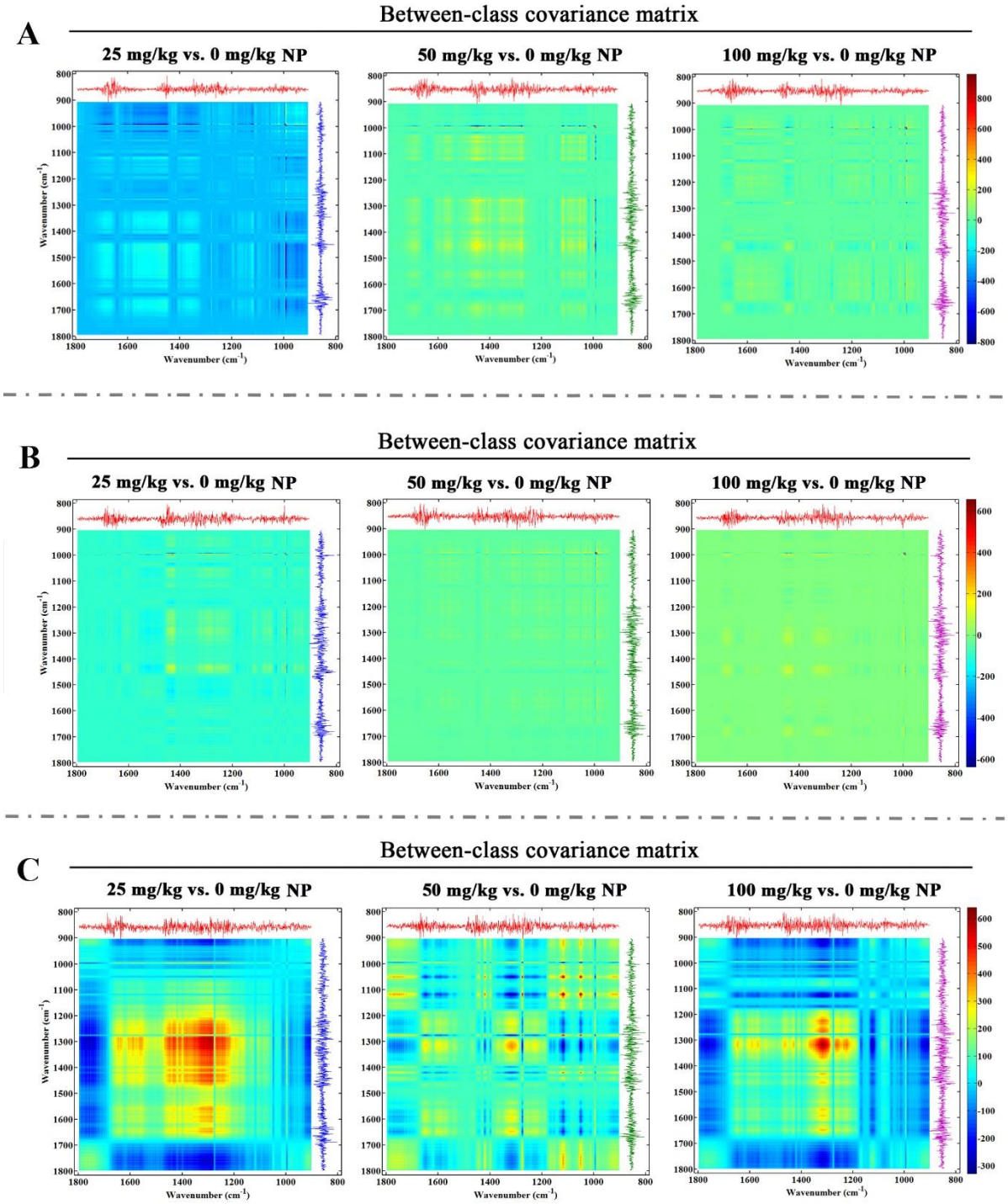

Figure S11. Raman spectroscopic-based between-class covariance matrix showing the absorbance variations of 4-nonylphenol (NP) treatment *vs.* control categories. Between-class covariance matrix of spectral region 1800-900 cm^{-1} for NP-treated 21-day-old rats **(A)**, for NP-treated 35-day-old rats **(B)** and for NP-treated 50-day-old rats **(C)**. Between group comparison: 25 mg/kg *vs.* 0 mg/kg NP groups, 50 mg/kg *vs.* 0 mg/kg NP groups and 100 mg/kg *vs.* 0 mg/kg NP groups. Data represent the average of six mice per group.

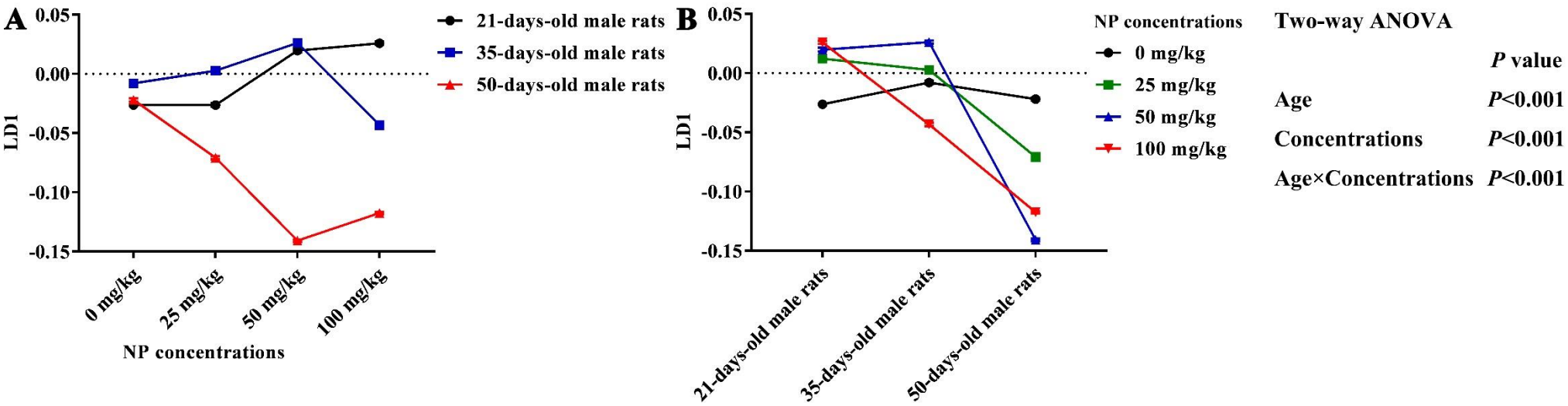

Figure S12. Linear discriminant 1 (LD1) score of Raman spectra extracted from testicular interstitial tissue was analysed by two-way ANOVA to evaluate the effect of exposure age, 4-nonylphenol (NP) administration, or interaction. The effect of NP-exposure life stage on LD1 scores of both the 1800-900 cm^{-1} region **(A)** and 3200-2800 cm^{-1} region **(B)**. The effect of NP exposure on LD1 scores of both the 1800-900 cm^{-1} region **(C)** and 3200-2800 cm^{-1} region **(D)**. Data represent mean ± 95% confidence intervals.

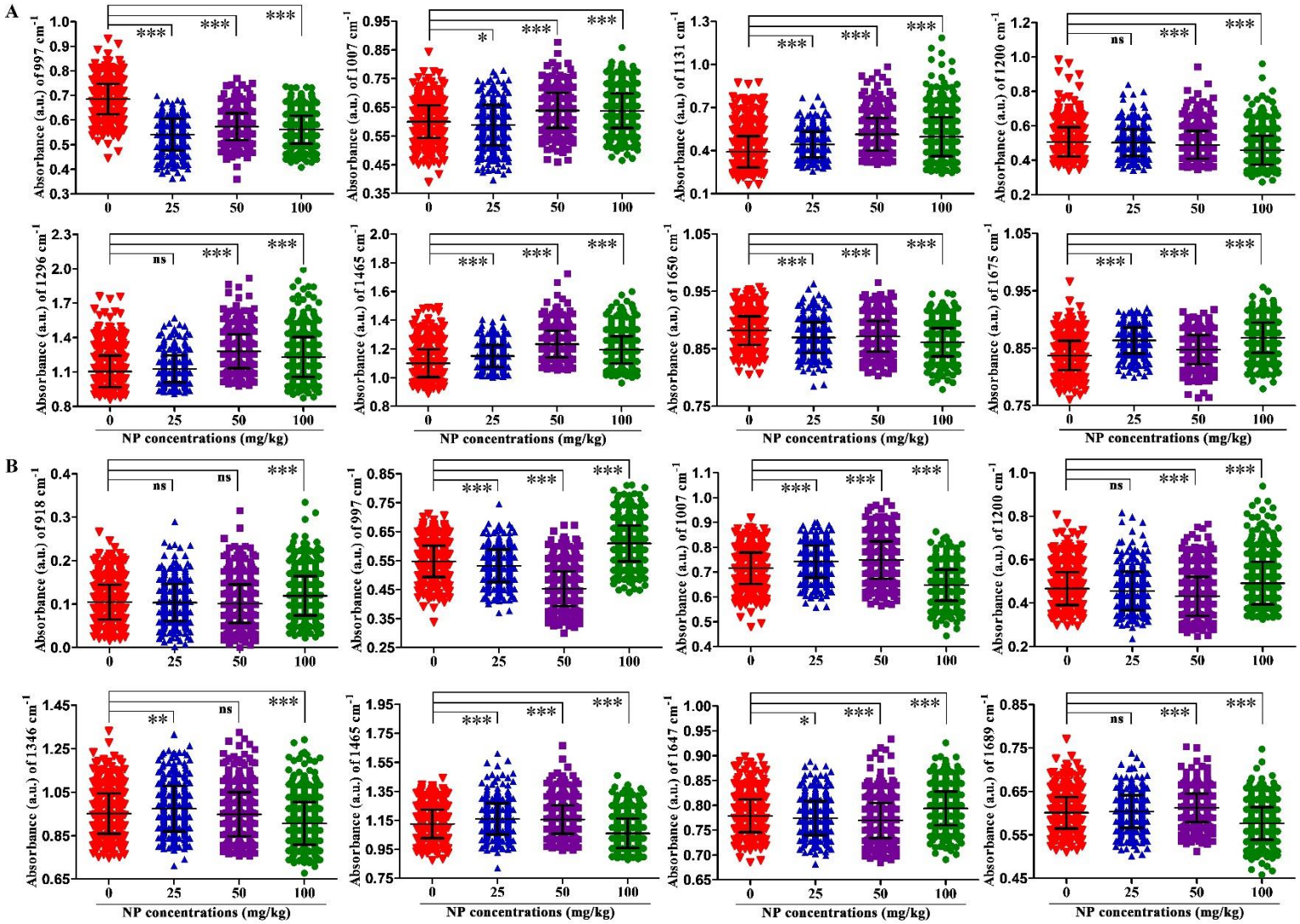
A
Absorbance (a.u.) of 997 cm-1
Absorbance (a.u.) of 1007 cm-1
Absorbance (a.u.) of 1131 cm-1
Absorbance (a.u.) of 1200 cm-1
Absorbance (a.u.) of 1296 cm-1
Absorbance (a.u.) of 1465 cm-1
Absorbance (a.u.) of 1650 cm-1
Absorbance (a.u.) of 1675 cm-1
NP concentrations (mg/kg)
B
Absorbance (a.u.) of 918 cm-1
Absorbance (a.u.) of 997 cm-1
Absorbance (a.u.) of 1007 cm-1
Absorbance (a.u.) of 1200 cm-1
Absorbance (a.u.) of 1346 cm-1
Absorbance (a.u.) of 1465 cm-1
Absorbance (a.u.) of 1647 cm-1
Absorbance (a.u.) of 1689 cm-1
NP concentrations (mg/kg)
0
25
50
100
ns
*
**
***

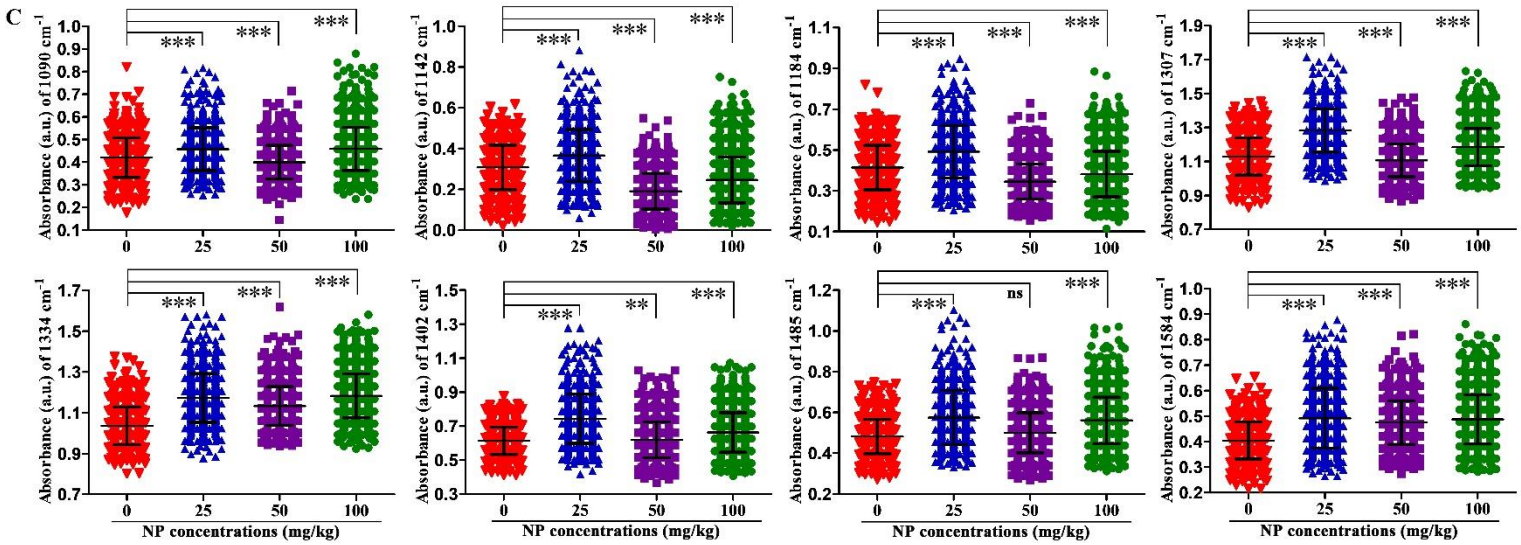

Figure S13. Variations of Raman spectral absorption of discriminating wavenumbers responsible for segregation of 4-nonylphenol (NP) exposure groups. (A) Absorption variations for the bands located at the 997, 1007, 1131, 1200, 1296, 1465, 1650 and 1675 cm^{-1} of testicular cells of NP-treated 21-day-old rats. **(B)** Absorption variations for the bands located at the 918, 997, 1007, 1200, 1346, 1465, 1647 and 1689 cm^{-1} of testicular cells of NP-treated 35-day-old rats. **(C)** Absorption variations for the bands located at the 1090, 1142, 1184, 1307, 1334, 1402, 1485 and 1584 cm^{-1} of testicular cells of NP-treated 50-day-old rats. All the data are represented as mean ± standard deviation, n=6 for each group. "ns" denotes no statistical significance (P>0.05); * indicates P-value of <0.05; ** indicates P-value of <0.01; *** indicates P-value of <0.001, one-way ANOVA with the Fisher's LSD or Dunnett's T3 post-hoc test.

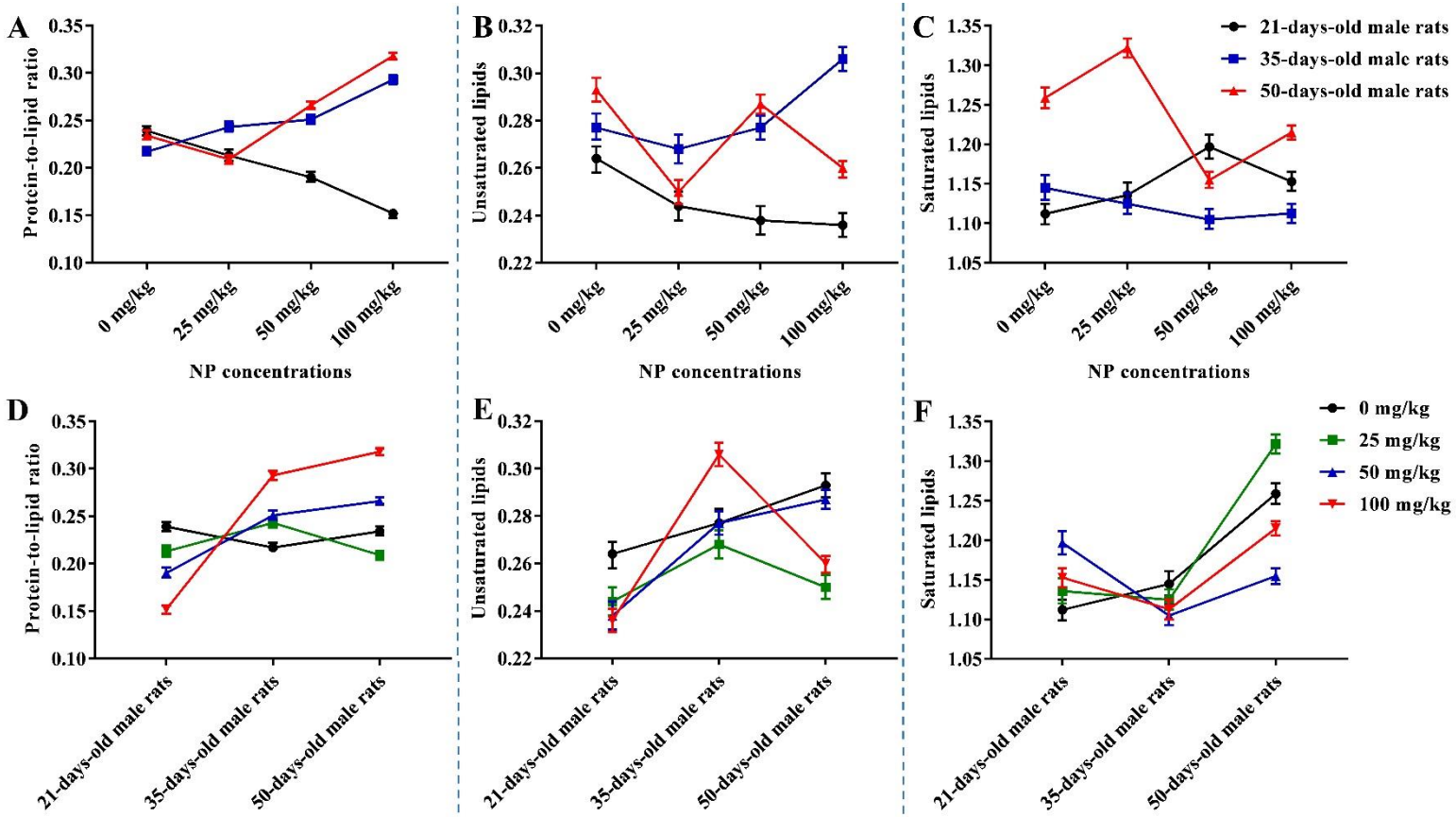

Two-way ANOVA

	P value
Ages	*P*<0.001
Concentrations	*P*<0.001
Age×Concentrations	*P*<0.001

Two-way ANOVA

	P value
Ages	*P*<0.001
Concentrations	*P*<0.001
Age×Concentrations	*P*<0.001

Two-way ANOVA

	P value
Ages	*P*<0.001
Concentrations	*P*<0.001
Age×Concentrations	*P*<0.001

Figure S14. The protein-to-lipid ratio, unsaturated lipids level and saturated lipids levels were analysed by two-way ANOVA to evaluate the effect of 4-nonylphenol (NP) administration, exposure age, or interaction. The effect of NP-exposure life stage on the protein-to-lipid ratio **(A)**, unsaturated lipids level **(B)** and saturated lipids level **(C)**. The effect of NP exposure on the protein-to-lipid ratio **(D)**, unsaturated lipids level **(E)** and saturated lipids level **(F).** Data represent mean ± 95% confidence intervals.

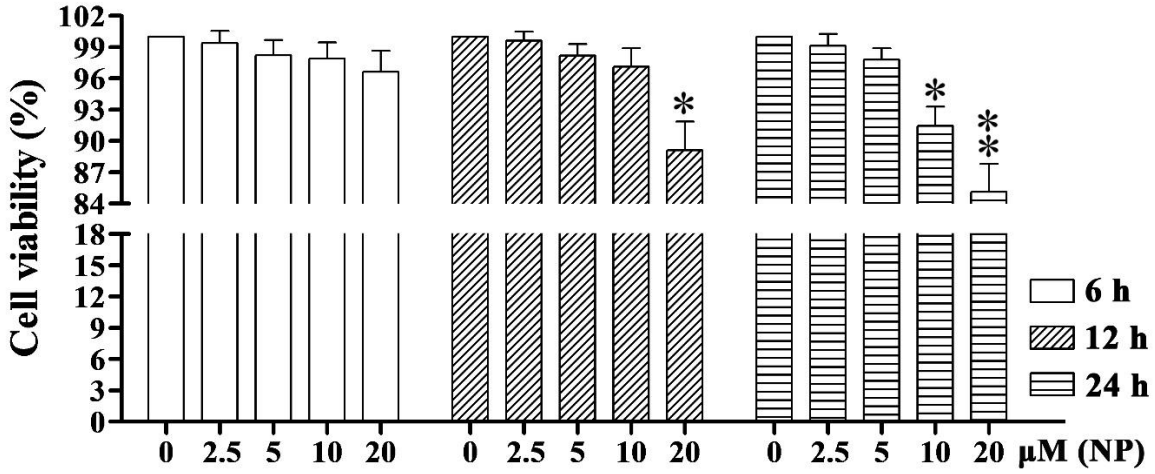

Figure S15. Effects of 4-nonylphenol (NP, 0-20 μM) on the cell viability of Sertoli cells (SCs) was assessed using the CCK-8 test. Primary SCs were treated with various concentrations of NP for 6, 12 and 24 h. SCs treated with only DMSO (0.01%, v/v) were used as control. The experiments were repeated six times, and the data presented as mean ± standard deviation. *$P<0.05$, **$P<0.01$ *vs.* control group (0 μM NP), one-way ANOVA with the Fisher's LSD or Dunnett's T3 post-hoc test.

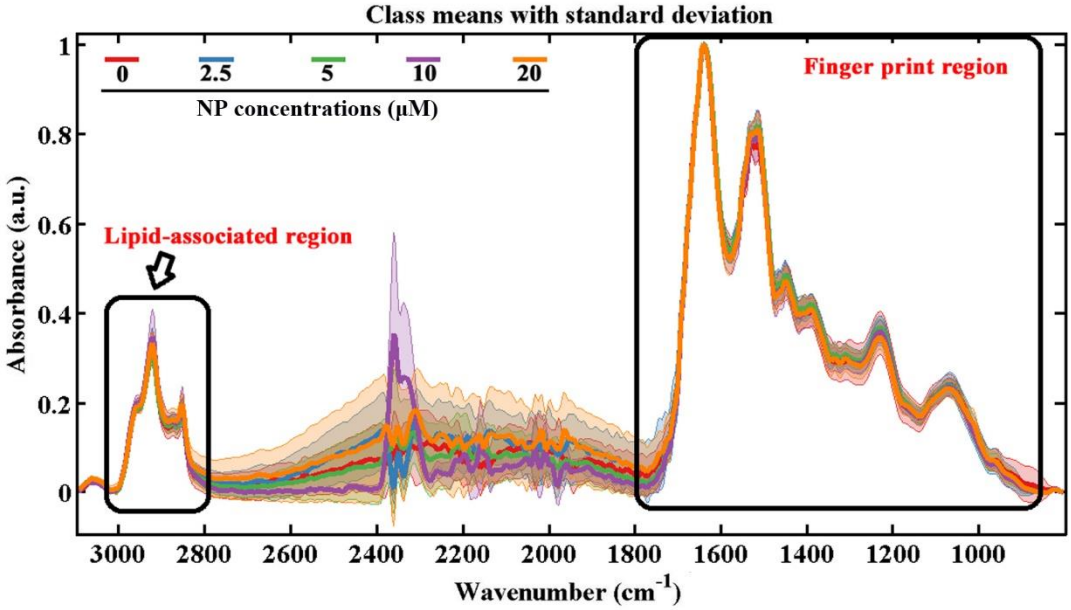

Figure S16. Mean IR spectra ± standard deviation derived in the analysis of Sertoli cells (SCs) in the 3100-800 cm^{-1} region. The resultant IR spectra included two regions of interest at 3200-2800 cm^{-1} (CH-region: lipids) and 1800-900 cm^{-1} (biochemical-cell fingerprint region). IR spectra were baseline-corrected and normalized to the Amide I. Primary SCs were treated with various concentrations of 4-nonylphenol (NP) for 12 h. The different categories were classified as: 0 μM NP (red solid line), 2.5 μM NP (blue solid line), 5 μM NP (green solid line), 10 μM NP (purple solid line), and 20 μM NP (yellow solid line). The experiments were repeated six times.

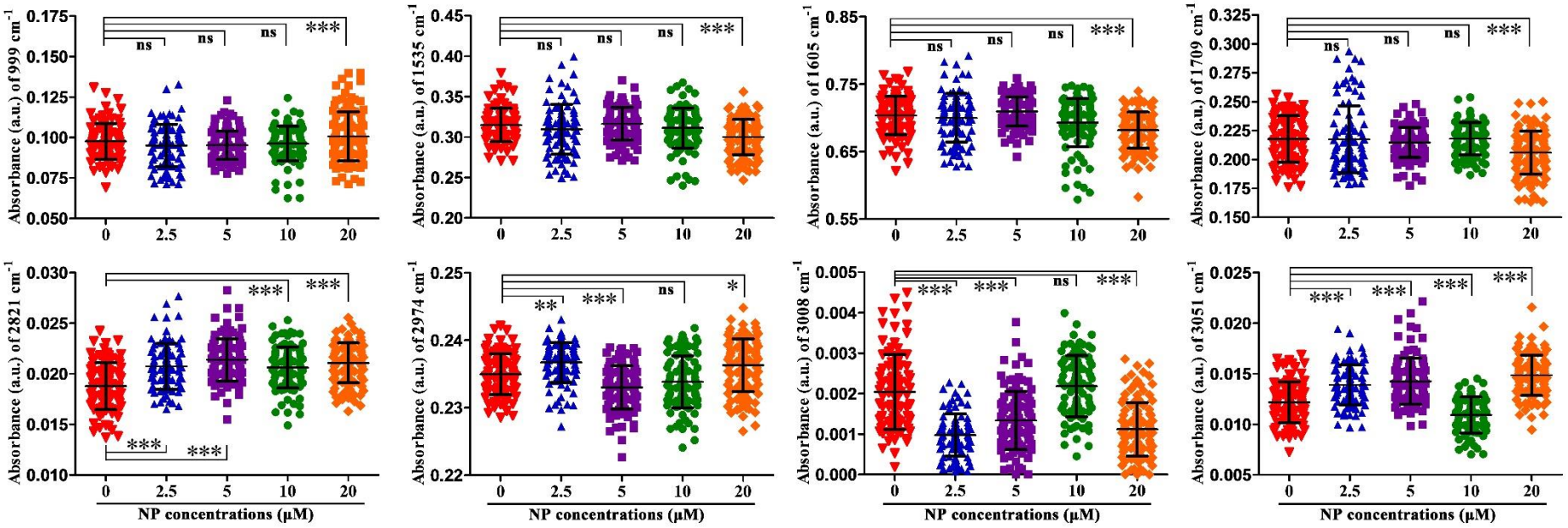

Figure S17. Variations for the IR spectral absorption bands located at the 999, 1535, 1605, 1709, 2821, 2974, 3008 and 3051 cm^{-1} of Sertoli cells treated with 4-nonylphenol (NP). All the data are represented as mean ± standard deviation. "ns" denotes no statistical significance (P>0.05); * indicates P-value of <0.05; ** indicates P-value of <0.01; *** indicates P-value of <0.001, one-way ANOVA with the Fisher's LSD or Dunnett's T3 post-hoc test.

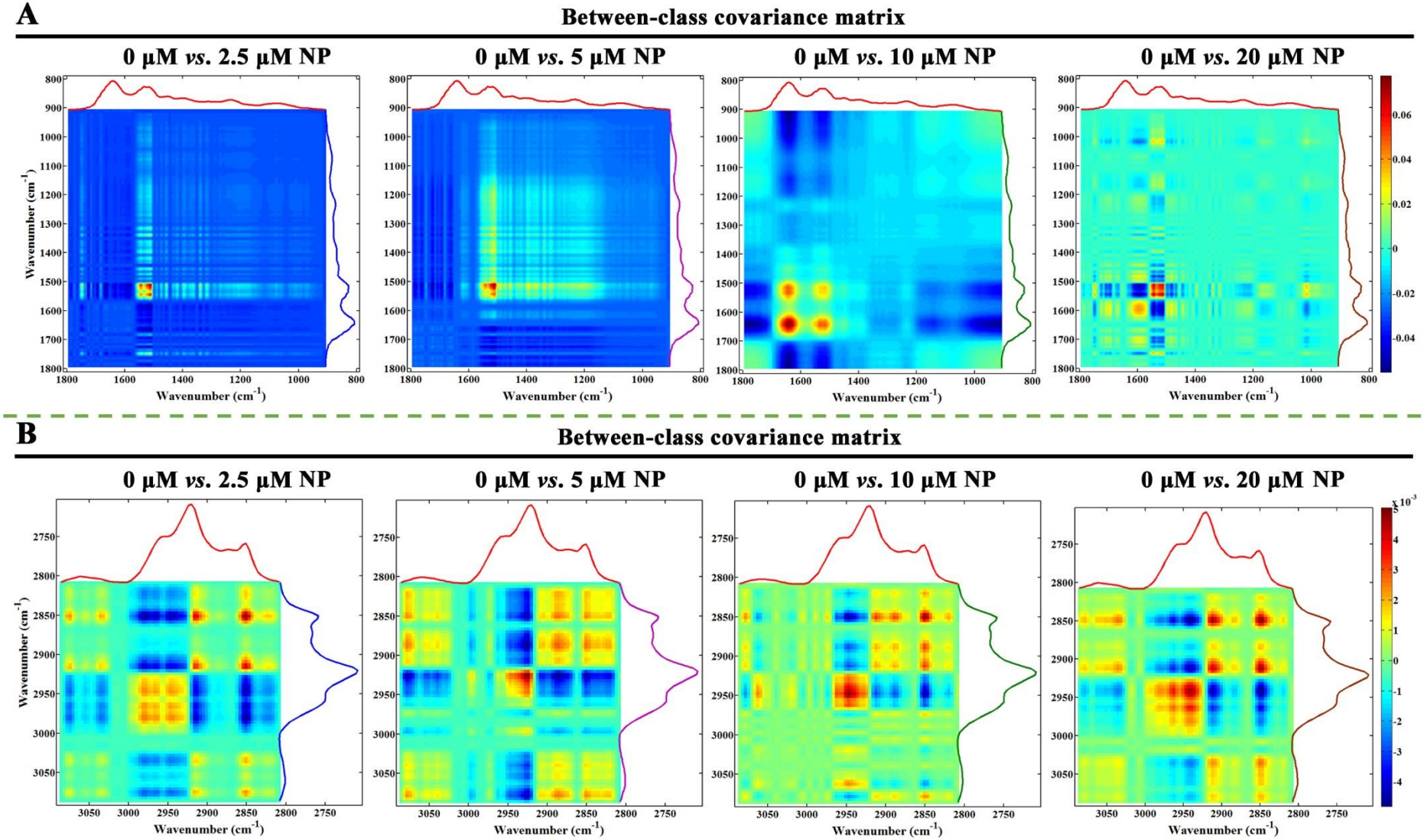
A
Between-class covariance matrix
0 µM vs. 2.5 µM NP
0 µM vs. 5 µM NP
0 µM vs. 10 µM NP
0 µM vs. 20 µM NP
Wavenumber (cm-1)
B
Between-class covariance matrix
0 µM vs. 2.5 µM NP
0 µM vs. 5 µM NP
0 µM vs. 10 µM NP
0 µM vs. 20 µM NP
Wavenumber (cm-1)

8 **Figure S18. ATR-FTIR spectroscopy-based between-class covariance matrix of spectral region 1800-900 cm^{-1} (A) and 3200-2800 cm^{-1} (B)**
9 **for Sertoli cells treated with 4-nonylphenol (NP).** Between-groups comparison: 0 μM *vs.* 2.5 μM NP groups, 0 μM *vs.* 5 μM NP groups, 0 μM
10 *vs.* 10 μM NP groups, and 0 μM *vs.* 20 μM NP groups.